

# A REVIEW OF METALLIC PHOTOCATHODE RESEARCH

Dr. D.T. Palmer, Ph.D.  
 Stanford Linear Accelerator Center  
 2575 Sand Hill Road  
 Menlo Park, California 94025, USA

Abstract

We have assumed that a Magnesium (Mg) photocathode can produce a quantum efficiency on the order of  $10^{-3}$ , which is based on a QE graph posted on the Brookhaven National Laboratory Accelerator Test Facility website. The link to this plot is listed below. This ARDB technical note is an attempt to understand where the data came from and under what experimental conditions the data was taken. Experiments conducted at the UCLA Neptune Laboratory on an exact copy of the ORION RF gun indicate that the Mg quantum efficiency (QE) is  $2.5 \times 10^{-5}$  using normal incidence and a laser injection phase of  $45^\circ$  with respect to the zero crossing [11]. [http://www.bnl.gov/atf/capfiles/photocat/quantum\\_eff.html](http://www.bnl.gov/atf/capfiles/photocat/quantum_eff.html).

## 1. INTRODUCTION

In this article, questions about the validity of the reference data for Magnesium (Mg) and Copper (Cu) photocathodes are investigated. This is due to our need for accurate data to estimate the maximum charge ( $Q_T$ ) that can be produced by the ORION Photoinjector.

The ORION Photoinjector consists of a 1.6 cell Photocathode RF gun, and it operates at 10 Hz with 30 MW of S-band peak RF power. An emittance compensation magnet is used to control emittance growth due to the linear space charge forces in the electron beam. The Ultraviolet (UV) drive laser system consists of a Spectra-Physics Millennia/Tsunami oscillator with an Evolution-30 Spitfire-HPR regenerative amplifier. A Tripler plate X3 is used to convert the Infrared Red light (IR) to Ultraviolet (UV) with an efficiency of 10%. The X3 Tripler is located in the ORION laser room. The output of the UV drive laser system, 2.3 mJ at 1 KHz at 800 nm, is transported to the RF gun via a relayed imaged vacuum transport system line. Three UV grade UHV windows are used to transport the UV laser light from the laser clean room to the photocathode. Two of these UV windows are used for the UHV laser transport line and the third is used to allow the UV laser pulse to enter the UHV RF gun with minimum loss of energy. The UV laser light transport system from the X3 Tripler plate to the photocathode will produce an energy loss that is dependent on the mode of operation of the ORION photoinjector.

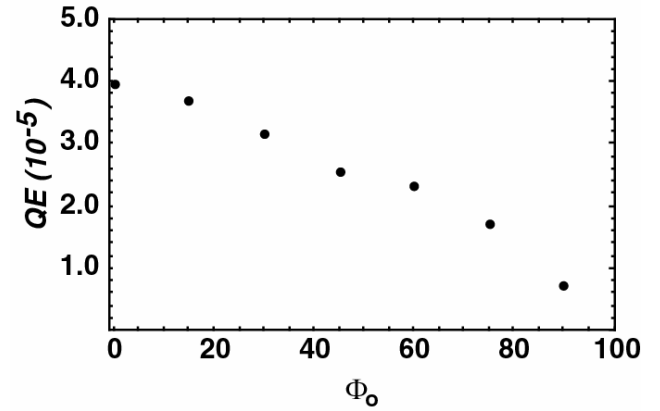
Table 1: Modes of operation and laser transport efficiency for the ORION UV laser system. **X** indicates the elements used for a given mode of operation.

| <i>Element</i>  | <i>Loss per Element</i> | <i># of elements</i> | <i>Total Efficiency</i> | <i>Mode 0</i><br><i><math>Q_T &gt; 1 \text{ nC}</math></i> | <i>Mode I</i><br><i><math>Q_T = 250 \text{ pC}</math></i> | <i>Mode II</i><br><i><math>Q_T = 50 \text{ pC}</math></i> |
|---|-------------------------|----------------------|-------------------------|--|---|---|
| Fourier LCD Mask (IR)                                 | 0.10                    | 1                    | 0.90                    |  | X   |   |
| Spatial LCD Mask (IR)                                 | 0.10                    | 1                    | 0.90                    |  | X   |   |
| Harmonic Converter (IR to UV)                         | 0.90                    | 1                    | 0.10                    | X  | X   | X   |
| Grating   | 0.25                    | 1                    | 0.75                    |  | X   | X   |
| Cylindrical Lens                                      | 0.10                    | 1                    | 0.90                    |  | X   | X   |
| Mirror  | 0.02                    | 15                   | 0.74                    | X  | X   | X   |
| Aperture  | 0.65                    | 1                    | 0.35                    |  |   |   |
| Polarizer   | 0.05                    | 1                    | 0.95                    | X  | X   | X   |
| Lens  | 0.02                    | 15                   | 0.74                    | X  | X   | X   |
| UHV Optical Port                                      | 0.08                    | 3                    | 0.78                    | X  | X   | X   |
| <i>Total efficiency per a given mode of operation</i> |                         |                      |                         | <i>0.0406</i>  | <i>0.0222</i>   | <i>0.0274</i>   |
| <i>Total Charge produced</i>                          |                         |                      |                         | <i>0.500 nC</i>  | <i>0.275 nC</i>   | <i>0.340 pC</i>   |

Mode 0 is the maximum charge case of  $> 1 \text{ nC}$ , Mode I is the design baseline or  $0.25 \text{ nC}$ , and Mode II is the E-163 case of  $50 \text{ pC}$ . The design bunch charge and the estimated UV efficiencies for a given mode of operation are delineated in Table 1 along with an estimated  $Q_T$  that a given mode of operation can produce. It should be noted that the IR Spatial LCD Mask and the aperture are devices to flatten the transverse profile of the UV laser beam and therefore only one of these technologies should be used at any given time.

Experimental results of our friction-welded Mg photocathode at a laser injection phase of  $45^\circ$  with respect to the zero crossing and the laser beam normal to the photocathode a  $QE = 2.5 \times 10^{-5}$  [10]. The peak field gradient was  $85 - 90 \text{ MV/m}$  and the vacuum level was  $1 \times 10^{-8} \text{ torr}$  with the RF on and  $2 \times 10^{-9} \text{ torr}$  with the RF off.

Figure 1: QE data for Mg versus laser injection phase,  $\Phi_o$ .



Assuming a laser injection phase of,  $\Phi_o = 45^\circ$ , to support both Mode I and II with a total charge of  $Q_T^I = 275$  pC and for Mode II  $Q_T^{II} = 340$  pC, for Mode 0 operation the maximum charge we will be able to produce is estimated to be  $Q_T^0 = 500$  pC. The Mode 0 limitation is the driving force to understand the smaller than expected Mg QE of  $2.5 \times 10^{-5}$  from our high power RF QE experiments conducted at UCLA [10].

It should be noted that UCLA data use a normal incidence laser, whereas the ORION Photoinjector will use one of two  $72^\circ$  grazing incidence laser ports. We suggest that the Mode 0 limitation in the total charge,  $Q_T^0$ , can be overcome by increasing  $\Phi_o$  from  $45^\circ$  to  $90^\circ$ . This will increase the QE from  $2.5 \times 10^{-5}$  to  $4.0 \times 10^{-5}$ , or the total charge will scale by 1.6 or 800 nC. In addition, the accelerating gradient,  $E_z$ , can be increased from 85 to 170 MeV/m, so the Schottky effect will be increased by a factor of  $\sqrt{2}$ . The ORION RF gun has been high power RF processed up to 16 MW peak power with a PRF of 10 Hz. [DTP] During this experiment, the RF macro pulse width was a  $3.5 \mu\text{s}$  square pulse, which corresponds to approximately 157 MeV/m through the device's shunt impedance of  $R_s = 40.98 \text{ M}\Omega/\text{m}$ . With these assumptions the ORION photoinjector will be able to support Mode 0 operation with a total charge,  $Q_T^0 = 1.13 \text{ nC}$ .

In Section 2 of the is technical note, we will find an increase in the QE by approximately a factor of 3 in the effective QE of Mg due to the use of p-polarized laser light at a  $72^\circ$  grazing incident angle [7]. This will allow the ORION photoinjector to produce up to 3.4 nC.

## 2. THEORY

Quantum efficiency (QE) is defined by the number of electrons,  $N_e$  produced divided by the number of photons,  $N_\gamma$  at a given wavelength.  $Q_T$  is electron bunch charge measured in units of nC, and  $E_\gamma$  is the laser pulse energy measured in units of  $\mu\text{J}$  at 266 nm.

$$QE = \frac{N_e}{N_\gamma} = 4.645 \times 10^{-3} \left[ \frac{\mu\text{J}}{\text{nC}} \right] \left[ \frac{Q_T}{E_\gamma} \right] \quad [1]$$

To first order, the quantum efficiency ( $\eta$ ) can be expressed [9] as in Equation 2, where  $\phi$  is the effective work function of the photocathode material.

$$\eta = A[h\nu - \phi]^2 \quad [2]$$

$$\phi_o - \phi = \left[ \frac{eE}{4\pi\epsilon_o} \right]^{1/2} \quad [3]$$

$$\eta^{1/2} = A^{1/2} \left[ h\nu - \phi_o + \left[ \frac{eE}{4\pi\epsilon_o} \right]^{1/2} \right] \quad [4]$$

$\phi_o$  is the zero field work function, E is the surface electric field, e is the electron charge, h is Plank's constant,  $\nu$  is the frequency of the incident laser light, A is a constant that is material dependent, and  $\epsilon_o$  is the dielectric constant of free space.

## 3. PAST EXPERIMENTAL RESULTS

Previous experimental results from CERN and Brookhaven Accelerator Test Facility (ATF) are reviewed in this ARDB Technical Note using Figure 1 as our point of reference. Three different photocathode materials are represented in Figure 1:  $\text{Cs}_2\text{Te}$ , Mg and Cu. We shall review only the Mg and Cu metal photocathode material in the following sections.

MAGNESIUM PHOTOCATHODE EFFICIENCIES  
VS. PHOTON ENERGY  
COMPARED TO Cu AND  $\text{Cs}_2\text{Te}$

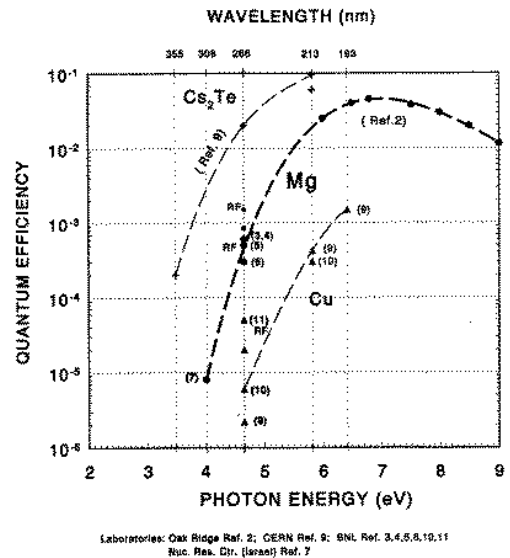


Figure 2: QE data for  $\text{Cs}_2\text{Te}$ , Mg, and Cu photocathodes versus wavelength [0].

[http://www.bnl.gov/atf/capfiles/photocat/quantum\\_eff.html](http://www.bnl.gov/atf/capfiles/photocat/quantum_eff.html).

### 3.1.1. Copper Quantum Efficiency Data [1]

The Copper (Cu) data in Figure 1 was taken at five different wavelength (193, 213, 266, 308, 355 nm) and using two different cleaning procedures. Some of the Cu data at longer wavelengths had been omitted by the graphical artist that produced Figure 1.

Ionized Controlled Etching (ICE) [2] was conducted on two samples at 193 nm and 213 nm. There was an increase in the QE with this cleaning method, as can be seen in Table 2.

Table 2: Copper Quantum Efficiency Data from CERN Reference [1].

| Wavelength<br>$\lambda$ (nm) | Copper<br>QE         | Reference |
|------------------------------|----------------------|-----------|
| 193                          | $2.0 \times 10^{-4}$ | 1         |
|                              | $1.5 \times 10^{-3}$ | 1, 2      |
| 213                          | $1.5 \times 10^{-4}$ | 1         |
|                              | $4.2 \times 10^{-4}$ | 1, 2      |
| 266                          | $2.2 \times 10^{-6}$ | 1         |
| 308                          | $1.6 \times 10^{-7}$ | 1         |
| 355                          | $8.0 \times 10^{-8}$ | 1         |

Table 3: Magnesium Quantum Efficiency Data from an RF Gun Reference [4].

| Wavelength<br>$\lambda$ (nm) | Magnesium QE         | RF Field<br>Gradient |
|------------------------------|----------------------|----------------------|
| 266                          | $2.5 \times 10^{-4}$ | 50 MV/m              |
| 266                          | $5.0 \times 10^{-4}$ | $\sim 70$ MV/m       |

### 3.1.2. Ionized Controlled Etching (ICE) [2]

Argon (Ar) gas with a purity of 99.9997% was used to produce the cleaning plasma. The internal pressure of the plasma vessel was  $5 \times 10^{-2}$  Torr. The cathode material was maintained at a DC potential of  $V_k: -0.5 \text{ KV} < V_k < -2.0 \text{ KV}$ . A magnetic field was used to confine the Argon Plasma. The plasma is generated using an arc discharge technique.

### 3.2. Magnesium Quantum Efficiency Data

The Accelerator Test Facility at the Brookhaven National Laboratory has investigated various metal photocathodes. In this section, we review their cleaning processes and quantum efficiency results for Magnesium and Copper.

Initial work at BNL/ATF using Mg as a photocathode was at normal incidence with a removable center plug approximately 25 mm in diameter with a 6 mm Magnesium disk pressed fit into its center. This removable cathode plug was polished with a one micron diamond paste. It should be noted that significant breakdown was observed and limited the maximum field gradient that the RF gun could attain [6]. The vacuum at the Mg cathode was estimated to be  $5 \times 10^{-7}$  Torr for the QE values reported in Table 3.

It is not possible to compare the data in Table 3 with Equation 4 due to the lack of laser energy data for both experiments.

But for constant laser pulse energy, as used in the Figure 5, we can see that as the cathode electric field strength is increased the bunch charge increases as expected from Equation 4.

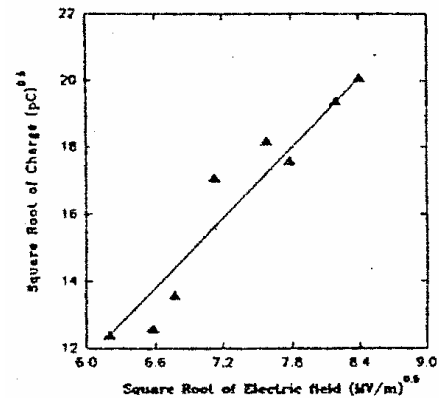


Figure 3: [5]. Square root of photoelectrons versus the square root of the applied cathode electric field, for constant laser pulse energy.

Photocathode preparation techniques have been the hall mark of the QE work conducted at BNL. The following is verbatim from reference [8].

*“The flat photocathodes are made of high-purity sheet metal disks, MACHINED from the desired metal. The disks are soldered to copper electrodes, which is then lapped with 1- $\mu\text{m}$  diamond compound, washed in solvents, ultrasonically cleaned, and stored in hexane topped with  $N_2$ . When setting the electrode gap, the photocathode experiences a brief 1 – 2 minutes exposure to air. The assembly is then cleaned under a  $N_2$  jet and installed in the test cell, which is filled with  $N_2$ . The cell is then evacuated, baked at  $\sim 150^\circ\text{C}$ , and pumped to a pressure of  $\sim 10^{-9}$  Torr at room temperature”*

DC measurements were conducted using a vacuum photodiode cell. The photocathodes are laser cleaned using a 10 Hz 266 nm (4.66 eV) laser beam with an energy density of 2-5  $\text{mJ}/\text{cm}^2$ . During the laser cleaning which lasts 5-10 minutes the following effects were observed.

1. QE increased, sometime by 4 orders of magnitude.
2. 1-eV and 2-eV photons are much less effective.
3. The pressure in the chamber increased during activation of the photocathodes.
4. As the QE decreased slowly as a function of time, the ambient pressure increased.

The measured multi-shot optical damage threshold for copper using a 10 Hz, 266 nm, 10 psec laser pulses was found to be 100 mJ/cm<sup>2</sup>. Therefore no damage was seen during the laser cleaning/ activation process.

Table 4: Magnesium and Copper Quantum Efficiency for a DC gun Reference [8].

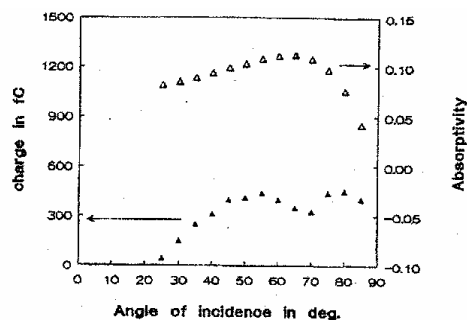
| Wavelength<br>$\lambda$ (nm) | Material | QE                    | DC Field<br>Gradient |
|------------------------------|----------|-----------------------|----------------------|
| 266                          | Mg       | $6.25 \times 10^{-4}$ | 12 MV/m              |
| 266                          | Cu       | $1.4 \times 10^{-4}$  | -----                |

In reference [7], a high purity magnesium photocathode was diamond turned to eliminate contamination due to polishing compounds. Before installation in the vacuum cell, the samples were analyzed with an Auger electron spectrometer and cleaned by ion bombardment. The sample was then maintained in an N<sub>2</sub> atmosphere, although a brief exposure to air was unavoidable during installation. Additional in situ cleaning was accomplished using 248 nm light at 5 MW/cm<sup>2</sup>. The test cell pressure was < 10<sup>-8</sup> torr. In this study the p-polarized laser was incident on the photocathode at an angle of 75° with respect to the cathode normal. The QE, under these conditions, was reported to be ~ 3 x 10<sup>-4</sup>. These were DC measurements and the gap spacing was 3 mm. No voltage potential was reported in reference [7].

### 3.2.1. S- And P- Polarized 266 nm versus the angle of incidence.

In reference [8] the authors calculated the absorption of S-polarized and P-polarized 266 nm laser light as a function of laser incidence with respect to the photocathode normal. As the angle of incidence of S-polarized light changes from 0° to 90°, the absorption at 266 nm decreased from 0.074 to 0. For p-polarized laser light at 266 nm, there is a maximum in the absorption, (0.122) at 65°, the Brewster angle for magnesium. Figure 4 shows the calculated absorption and measured electron yield as a function of the angle of incidence for P-polarized radiation. The absorption data in Figure 4 indicates that irradiating the Mg photocathode near the Brewster angle will result in the electron yield being near the maximum.

Figure 4: [8]. Calculated absorption and measured electron yield as a function of the angle of incidence for p-polarized radiation.



### 3.2.2. Sputtered Magnesium [5]

A copper substrate was cleaned by ion bombardment and a 20µm thick layer of Mg was sputtered on to the copper substrate in a vacuum system with a pressure of 2 x 10<sup>-7</sup>. The coated substrate was shipped in a sealed argon container. Koral Labs, Inc., MN was the vendor that accomplished this coating.

During installation into the test chamber the samples were briefly exposed to air. Four samples were received.

One sample was polished with 1-µm diamond compound, rinsed in hexane and cleaned in an ultrasonic bath before being installed in the test chamber. The remaining samples remained unpolished. Two samples were baked out at ~100°C for 48 hours. One sample was baked out at 150°C. Each of the samples was irradiated for 12 hours with a UV lamp with an anode voltage of +7KV and with an anode cathode parallel separation of 3 mm. This corresponds to a field gradient of 2.33 MV/m. The vacuum level was on the order of 10<sup>-9</sup> torr. This procedure removes adsorbed gases effectively and results in highly reproducible cathodes.

### 3.2.3. Laser Cleaning of Sputtered Mg

At normal incidence the laser spot was ~300 µm full width at half maximum (FWHM) at normal incidence. An area of 1.0 mm x 1.5 mm was scanned at a 70° incidence angle for 90 min. The QE of an unpolished sample changed from ~2 x 10<sup>-5</sup> to ~2 x 10<sup>-3</sup>. This is a two order of magnitude change in the sputtered Mg QE.

The effect of laser scanning on the cathode material was studied using a mass spectrometer. After a 120°C bakeout the pressure was 5 x 10<sup>-9</sup> torr. The baseline mass spectrometer reading before laser scanning showed H<sub>2</sub>O, N<sub>2</sub>, H<sub>2</sub>, and CO<sub>2</sub>. The surface of the sample was scanned with an energy density of 600 µJ / mm<sup>2</sup> for 75 minutes. During the first 15 minutes the mass spectrum was dominated by the 40 atomic mass units (amu) line corresponding to MgO. During the next 5 minutes lines at 25, 26, and 27 amu dominated. These lines correspond to Mg, MgH, MgH<sub>2</sub>. At steady state the ratio of Mg to MgO signals was 3:1. It is the AUTHOR'S HYPOTHESIS is that Mg compounds are being formed with residual gases in the system while the Mg is being transported to the mass spectrometer.

### 3.2.4. Argon Sputtering of Sputtered Mg [5]

After laser cleaning of the above sample, additional cleaning using argon ion bombardment was used for 15 seconds which removed 100 Å of the sample. An Auger Spectrum of the surface was taken which indicated the presence of Mg, Cl, and O<sub>2</sub>. The 15 sec argon ion bombardment, auger spectrum cycle was repeated until the Cl and O<sub>2</sub> line disappeared and the Mg line dominated. This took approximately 1500Å or 15 cycles to accomplish. These results indicate that combining laser cleaning (300 μJ/mm<sup>2</sup> for 90 minutes versus 75) with argon ion sputtering can produce a pure Mg photocathode without creating deep damages on the photocathode surface.

### 3.2.5. Damage Threshold Studies

A 10 Hz, 266 nm, ~12 psec laser pulse with a laser spot size of 300 μm full width at half maximum (FWHM) was used in these studies. The laser energy density was increased from 100 μJ/mm<sup>2</sup> to 7.5 mJ/mm<sup>2</sup>. Each site received 3000 laser shots. Using X30 magnification indicates that for < 200 μJ/mm<sup>2</sup> there were no visible marks on the surface. For an energy density between 200 μJ/mm<sup>2</sup> and 350 μJ/mm<sup>2</sup>, the irradiated area was **distinguishable** from the un-irradiated area. Beyond this energy density, visible changes to the irradiated surface were linked to changes to the surface structure. At an energy density of 600 μJ/mm<sup>2</sup> small craters with a depth of ~ 1 μm were observed using a microscope with x100 magnification.

## 4. CONCLUSIONS

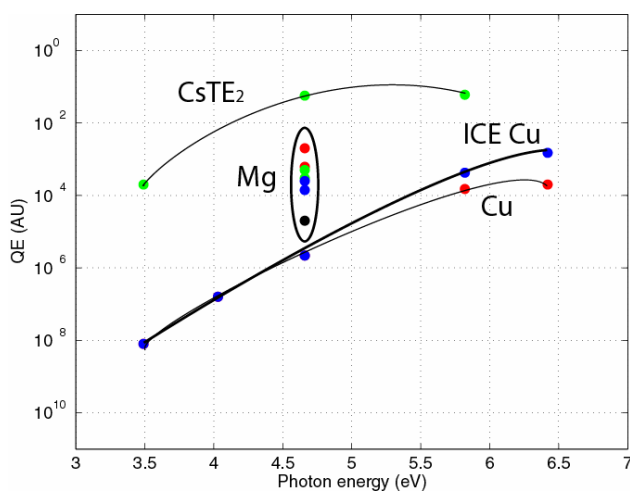


Figure 5: Compiled data from this literature search.

## 5. ACKNOWLEDGMENTS

The author would like to thank Professor Robert H. Siemann for his suggestion that I pursue this area of research.

## Reference

1. [http://www.bnl.gov/atf/capfiles/photocat/quantum\\_eff.html](http://www.bnl.gov/atf/capfiles/photocat/quantum_eff.html).
2. E. Chevallay, et al., "PHOTOCATHODES TESTED IN THE DC GUN OF THE CERN PHOTOEMISSION LABORATORY", Workshop on High Intensity Electron Sources, Legnaro Padova, Italy 24-28 May 1993, CERN/PS 93-22 (LP), CLIC Note 203
3. M. Wurgel, "NETTOYAGE IONIQUE SOUS VIDE DES PHOTOCATHODES" PS/LP Technique N<sup>o</sup> 91-03, Janvier 1991, CERN
4. F. Zhou, et al., "Experimental characterization of emittance growth induced by nonuniform transverse laser distribution in a photoinjector", Physical Review Special Topics – Accelerators and Beams, Volume 5, 094203 (2002)
5. X.J. Wang, et al., "Photoelectrons Beam Measurement from a Magnesium Cathode in a RF Electron Gun", LINAC 1994
6. T. Srinivasan-Rao, et al., "Sputtered magnesium as a photocathode material for rf injectors", Review of Scientific Instruments, Volume 69, Number 6, June 1998
7. X.J. Wang, et al., "Design and Construction a Full Copper Photocathode RF Gun", Proceedings of the 1993 Particle Accelerator Conference, Volume 4 of 5, Page 3000-3003
8. T. Srinivasan-Rao, et al., "Photoemission from Mg irradiated by short pulse ultraviolet and visible lasers", J. Appl. Phys. **77** (3) 1 February 1995
9. T. Srinivasan-Rao, et al., "Photoemission studies on metals using picosecond ultraviolet laser pulses", J. Appl. Phys. **69** (5) 1 March 1991
10. M. Cardona and L. Ley, in *Photoemission in Solids*. Edited by M. Cardona and L. Ley (Springer, New York, 1978), p. 23
11. D. T. Palmer, J. B. Rosenzweig, and J. England *Private communications*
12. D. T. Palmer and J. B. Rosenzweig, AAC200

